Breast Cancer Res Treat
DOI 10.1007/s10549-014-2887-9

PRECLINICAL STUDY

Primary breast tumor-derived cellular models: characterization of tumorigenic, metastatic, and cancer-associated fibroblasts in dissociated tumor (DT) cultures

Katherine Drews-Elger · Joeli A. Brinkman · Philip Miller · Sanket H. Shah · J. Chuck Harrell · Thiago G. da Silva · Zheng Ao · Amy Schlater · Diana J. Azzam · Kathleen Diehl · Dafydd Thomas · Joyce M. Slingerland · Charles M. Perou · Marc E. Lippman · Dorraya El-Ashry

Received: 15 November 2013 / Accepted: 14 February 2014

Abstract Our goal was to establish primary cultures from dissociation of breast tumors in order to provide cellular models that may better recapitulate breast cancer pathogenesis and the metastatic process. Here, we report the characterization of six cellular models derived from the dissociation of primary breast tumor specimens, referred to as "dissociated tumor (DT) cells." In vitro, DT cells were characterized by proliferation assays, colony formation assays, protein, and gene expression profiling, including PAM50 predictor analysis. In vivo, tumorigenic and metastatic potential of DT cultures was assessed in NOD/SCID and NSG mice. These cellular models differ from recently developed patient-derived xenograft models in that they can be used for both in vitro and in vivo studies. PAM50 predictor analysis showed DT cultures similar to their paired primary tumor and as belonging to the basal and Her2-enriched subtypes. In vivo, three DT cultures are tumorigenic in NOD/SCID and NSG mice, and one of these is metastatic to lymph nodes and lung after orthotopic inoculation into the mammary fat pad, without excision of the primary tumor. Three DT cultures comprised of cancer-associated fibroblasts (CAFs) were isolated from luminal A, Her2-enriched, and basal primary tumors. Among the DT cells are those that are tumorigenic and metastatic in immunosuppressed mice, offering novel cellular models of ER-negative breast cancer subtypes. A group of CAFs provide tumor subtype-specific components of the tumor microenvironment (TME). Altogether, these DT cultures provide closer-to-primary cellular models for the study of breast cancer pathogenesis, metastasis, and TME.

Keywords Primary cultures · Tumors · ER-negative breast cancer · Metastatic xenograft models

Abbreviations

DT	Dissociated tumor cells
CAF	Cancer-associated fibroblasts
ERα	Estrogen receptor alpha
TME	Tumor microenvironment

K. Drews-Elger · J. A. Brinkman · P. Miller · S. H. Shah · T. G. da Silva · Z. Ao · D. J. Azzam · J. M. Slingerland · M. E. Lippman · D. El-Ashry (✉)
Sylvester Comprehensive Cancer Center, Department of Medicine, University of Miami Miller School of Medicine, Biomedical Research Building, 1501 NW 10th Avenue, Miami, FL 33136, USA
e-mail: del-ashry@med.miami.edu

P. Miller · S. H. Shah
Sheila and David Fuente Graduate Program in Cancer Biology, University of Miami Miller School of Medicine, Miami, FL, USA

J. C. Harrell · C. M. Perou
Department of Genetics, University of North Carolina at Chapel Hill, Chapel Hill, NC 27599, USA

T. G. da Silva
Department of Surgery, University of Miami Miller School of Medicine, Miami, FL 33136, USA

A. Schlater
Division of Hematology/Oncology, Department of Internal Medicine, University of Michigan Medical Center, Ann Arbor, MI 48109, USA

K. Diehl
Department of Surgery, University of Michigan Medical Center, Ann Arbor, MI 48109, USA

D. Thomas
Department of Pathology, University of Michigan Medical Center, Ann Arbor, MI 48109, USA

Published online: 25 February 2014

EMT	Epithelial mesenchymal transition
IHC	Immunohistochemistry
FAP	Fibroblast activation protein
α-SMA	Alpha smooth muscle actin
TN	Triple-negative

Introduction

Breast cancer is the leading cause of cancer amongst women in the westernized world and mortality rates are greatly increased by the development of metastatic disease. In the United States, breast cancer is the most commonly diagnosed cancer and is the second leading cause of cancer-related deaths in women [51]. An important prognostic indicator in breast cancer is the presence or absence of estrogen receptor-α (ERα) in tumors. Approximately 30–40 % of breast cancers lack detectable ER protein and are thus resistant to endocrine therapies, and tend to have a worse prognosis than ER-positive breast cancers [13, 22, 41]. Moreover, an accumulating amount of data supports the classification of breast cancer into several molecular subtypes with characteristic gene expression profiles. This classification has revealed key differences amongst breast cancer subtypes and their correlation with clinico-pathologic features and response to treatment [4, 14, 15, 48]. One of the classifiers of the intrinsic subtypes, defined as the PAM50 predictor analysis, classifies breast cancer into five subtypes: luminal A, luminal B, normal-like, Her2-enriched, and basal-like [42, 52, 53]. More recently, the claudin-low subtype, identified within ER− basal tumors, has been described [44].

Currently, the study of early stage and metastatic breast cancer relies heavily on the use of established cell lines that are often derived from metastatic lesions rather than from primary tumors, limiting our understanding of primary tumor development. Nonetheless, these established cell lines have been widely used as cellular models of breast cancer as they are easy to handle and to replace from frozen stocks [11]. Additionally, because they are such a rich source of homogeneous, easily propagated material, they provide an excellent tool for molecular and cellular characterization of cancer pathogenesis studies requiring large cell populations and have contributed immensely to the understanding of the biology of breast cancer [28, 30]. However, there are several inherent disadvantages in using established cell lines as in vitro and in vivo models for breast cancer research. One issue lies in the fact that most breast cancer cell lines are derived from metastatic lesions such as pleural effusions, and may not reflect important aspects of the biology of the primary tumor [55]. The metastatic origin of most breast cancer cell lines brings into question their relationship to the primary tumor, as the latter are heterogeneous populations of cells and breast cancer cell lines trend to be more homogeneous populations. In addition, studying the mechanisms governing the metastatic process in its entirety is not always feasible with these types of cellular and xenograft models, as in most cases the primary tumor needs to be excised, or breast cancer cells must be introduced into host mice via tail vein or cardiac injection. While this approach has allowed a better understanding of metastasis, this method may unintentionally enhance the efficiency of colonization and does not fully recapitulate the complete metastatic process [16, 17], including crucial interactions of the tumor cells with tumor stroma.

It is becoming increasingly clear that cells from the tumor microenvironment (TME) including immune cells, pericytes, cancer-associated fibroblasts (CAFs), adipocytes, and endothelial cells play a vital role in tumor progression and metastasis [37, 20]. CAFs form an integral component of the TME, and are one of the major components of breast tumors [39]. These cells have been shown to originate from a variety of sources including bone-marrow mesenchymal stem cells (MSCs), local tissue fibroblasts, and even from cancer cells that have undergone an EMT process [5, 46, 54]. Regardless of their origin, CAFs have been shown to be involved in tumor initiation and progression [33], epithelial to mesenchymal transition and invasion (EMT) [8, 9, 56], angiogenesis [2, 3, 25, 40, 60], and metastasis, as well as conferring drug resistance [29, 50, 57]. Thus, use of cellular models of CAFs in the context of breast cancer biology may lead to the better understanding of crucial interactions within primary breast tumors.

Given that the scope of primary tumor heterogeneity and consequently the early stages of breast tumorigenesis are under-represented by current in vitro and in vivo models in breast cancer research, our purpose here was to establish patient-derived primary, short-term cultures from dissociation of specimens from breast tumors in order to provide cellular models that may better recapitulate breast cancer pathogenesis and metastasis.

Methods

Tumor dissociation and cell culture

Tumor specimens were obtained from surgical patients through the Tissue Procurement Core of the University of Michigan Comprehensive Cancer Center under a blanket IRB for prospective research and were de-identified prior to receipt. The tumors were not collected specifically for the currently proposed research project through an

interaction or intervention with living individuals, and samples were obtained from de-identified material. Dissociation of cells was performed as previously described [6]. Briefly, tumors were minced into small pieces with scalpel and dissociated in serum-free modified IMEM (Invitrogen) supplemented with 300 U/ml collagenase type 3 (Worthington Biochemical), 100 U/ml hyaluronidase (Worthington Biochemical), 2 % bovine serum albumin fraction V (Sigma), and 5 μg/ml recombinant human insulin (Sigma) at 37 °C, 5 % CO_2 with gentle agitation for 5–16 h until a majority of the tissue was digested. The dissociated cells were spun at $100\times g$ for 5 min and the cell pellet was plated into modified IMEM supplemented with 10 % FBS, 5 μg/ml recombinant human insulin (Invitrogen), and 50 μg/ml gentamicin (Invitrogen). Cells were grown at 37 °C, 5 % CO_2 forced-air humidified incubator, passaged continuously by detachment with 0.05 % trypsin (Invitrogen) and 0.53 mM EDTA (Sigma) until only tumor cells remained. At this point, cultures were named dissociated tumor (DT) and were grown in modified IMEM supplemented with 10 % FBS (HyClone). Human mammary fibroblasts (HMFs) were purchased from ScienCell (Cat. 7630) and cultured following manufacturer's instructions.

Animal studies: mammary fat pad injection and immunohistochemistry

Animal studies were performed following the approved protocol from the Institutional Animal Care & Use Committee (IACUC) at the University of Miami. Six- to eight-week-old female NOD/SCID and NSG mice were purchased from Jackson Laboratories. Cells were subcutaneously injected into the mammary fat pad and tumor formation of 1×10^6 DT cells on mammary fat pads 4 or 9 was assessed. For injection, cells were resuspended in 300 μl of collagen I–matrigel (1:1) solution (BD Biosciences). Body weight and tumor growth were monitored twice a week. The estimated volume was calculated by the formula: volume $= 0.4 \times L \times W^2$ (where L: length, W: width). Animals were euthanized when tumors reached 5 % of their total body weight. Tissues were collected, fixed in formalin, and paraffin embedded at the Division of Comparative Pathology at the University of Miami, Miller School of Medicine. Staining of harvested mouse tissues was performed at Lombardi Comprehensive Cancer Center, Georgetown University.

Microarray analysis

Total RNA was isolated using the miRNeasy kit (Qiagen) following manufacturer's instructions. After elution, RNA was DNAse treated (Epicentre Biotech). Microarray gene expression assays were performed at the University of North Carolina using Agilent 4×44 K custom arrays as previously described [24]. Intrinsic subtypes of our new samples were identified by including these microarrays with the UNC337 microarrays and then applying the PAM50 classifier [42] and claudin-low predictor [44]. Comparisons of pairwise gene expression were performed using the R statistical software v2.15.2. Microsoft Excel 2007, Microsoft Powerpoint 2007, and R statistical software v2.15.2 were used for figure generation [47].

Growth assays

For anchorage-dependent assays, cells were trypsinized and 12,500 cells were plated into triplicate wells of a 6-well plate. After allowing cells to plate for 24 h, an initial cell count was performed to assess the day 0 counts. Cell counts were performed every 2 days by trypan blue dye exclusion assay. Triplicates were averaged and plotted. Doubling times were calculated from values obtained from the linear portion of the growth curve using the equation: doubling time (h) $= (t_2 - t_1)/3.32(\log N_2 - \log N_1)$; where $t =$ time, N_2 is the average number of cells at t_2, and N_1 is the average number of cells at t_1.

Flow cytometry: cell cycle distribution and surface marker analysis

Asynchronously growing cells were fixed in 70 % ice-cold ethanol and kept at −20 °C overnight. Cells were then washed with PBS and labeled with propidium iodide staining solution (Sigma) and analyzed with a Fortessa flow cytometer and FlowJo software (BD Bioscience). Experiments were performed in three to six biological replicates of each of the DT cells. For surface marker analysis, cells were blocked for 20 min in 1× PBS containing 3 % fetal bovine serum (FBS). Cells were then incubated with surface marker-specific antibodies: PE mouse anti-human CD24 (BD Pharmingen) and APC mouse anti-human CD44 (BD Pharmingen) in the same solution and analyzed with a FACScan flow cytometer (BD Bioscience) and FlowJo software. Experiments were performed in three to six biological replicates of each of the DT cells.

Mammosphere formation assay

Mammocult® Human Medium kit was purchased from Stem Cell Technologies. Assay was performed following manufacturer's instruction. Briefly, 1×10^4 single cells were resuspended in 2 ml Mammocult® media plus proliferation supplements (StemCell tecnologies) and plated into ultra-low-attachment 6-well plates and incubated at 37 °C and 5 % CO_2. Mammospheres were counted after 6 days.

Soft agarose colony formation assay

A total of 2×10^4 cells/well were resuspended in 0.35 % agarose IMEM medium [supplemented with 10 % FBS, penicillin/streptomycin (Cellgrow) and fungizone (Sigma), and were seeded on top of a 0.6 % agarose (Invitrogen) IMEM (supplemented with 10 % FBS, penicillin/streptomycin and fungizone] layer in 6-well plates. All wells were monitored microscopically to assure single cell plating. The cultures were maintained at 37 °C, 5 % CO_2 atmosphere for up to 8 weeks, after which cell colonies were stained with crystal violet dye (Sigma) and counted. For co-culture experiments, 5×10^3 tumorigenic DTs were seeded either on their own or co-cultured with 15×10^3 cells of the CAF cultures.

Protein sample preparation, western blot analysis, and antibodies

Cells were homogenized in cold lysis buffer and processes as previously described [7]. Membranes were incubated overnight at 4 °C with the following primary antibodies diluted in 3 % bovine serum albumin: anti-Erb2 (Abcam), cytokeratin 19, cytokeratin 18, anti-EGFR (Cell Signaling), anti-vimentin (BD biosciences), and anti-alpha smooth muscle actin (Sigma). Membranes were washed with TBS-T and incubated with secondary antibody (diluted in blocking buffer) for 1 h at room temperature. The following secondary antibodies were used: ECL mouse IgG, HRP-linked whole antibody and ECL rabbit IgG, and HRP-linked whole antibody (Amersham). Membranes were washed with TBS-T and chemiluminescent detection was performed using SuperSignal West Pico substrate (Pierce).

Immunofluorescence

DT19, DT21, DT23, HMFs, and MCF7 cancer cell lines were immunofluorescently labeled for fibroblast activation protein (FAP), vimentin, pan-cytokeratin (CK), and Alpha-smooth muscle actin (α-SMA). For immunofluorescence staining, cells were harvested and plated onto cover glasses (VWR Intl, LLC). When cells reached 70 % confluency, they were fixed using 10 % formalin (Sigma-Aldrich, Co., St Louis, MO) for 10 min. After fixation, the coverslips were washed with 1× PBS (Gibco), and blocked with blocking buffer [5 % normal goat serum (Rockland, Gilbertsville, PA), 0.3 % Triton X-100 (Biorad, Hercules, CA)] for 1 h at room temperature. The cells were then subjected to primary and secondary antibody incubation. For FAP staining, the cells were incubated with anti-human FAP antibodies (eBioscience, San Diego, CA) for 1 h at room temperature, followed by 1× PBS wash. Secondary antibody incubation was done using Alexa Fluor® 488 goat anti-mouse IgG (Life Technologies) for 1 h at room temperature. For pan-cytokeratin staining, the cells were incubated with anti-human pan-cytokeratin antibodies (Dako North America, Inc., Carpinteria, CA) overnight at room temperature, followed by 1× PBS wash. Secondary antibody staining was done using Alexa Fluor® 488 goat anti-rabbit IgG (Life Technologies) overnight at room temperature. For vimentin staining, the cells were incubated with anti-human vimentin antibodies (Cell Signal) for 1 h at room temperature, followed by 1× PBS wash. Secondary antibody incubation was done using Alexa Fluor® 488 Goat Anti-Rabbit IgG (Life Technologies) for 1 h at room temperature. For α-SMA staining, the cells were incubated with anti-human α-SMA antibody (R&D Systems) for 1 h at room temperature, followed by 1× PBS wash. Secondary antibody incubation was done using Alexa Fluor® 488 goat anti-mouse IgG (Life Technologies) for 1 h at room temperature. After secondary antibody incubation, the cells were washed with 1× PBS (Gibco) and mounted onto slide with ProLong® Gold Antifade Reagent with DAPI (Life Technologies). Images were taken at 400× magnification using Zeiss Imager M1 microscope and pseudo-coloring was done using Nuance software.

Results

Tissue dissociation and generation of dissociated tumor (DT) cultures

Eight de-identified specimens of grade 3 primary breast tumors were obtained from surgical procedures and successfully dissociated into primary cultures. Specimens were from primary breast tumors belonging to ER−/PR−/H_2N− ($n = 3$), ER−/PR−/H_2N+ ($n = 2$), and ER+/PR−/H_2N+ ($n = 1$) (Table 1). Upon receipt, tissues were minced and placed in media containing dissociation enzymes (dissociation media) until the majority of the tissue was dissociated. This suspension was centrifuged at a low speed and the cell pellet was placed in culture and allowed to reach confluence, then detached and passaged (Fig. 1a). In the initial establishment of these cell cultures, there was more than one cell type present, and once one cell type predominated frozen stocks were prepared at different passages. These cell cultures are hereafter referred to as "dissociated tumor" (DT) cultures. All experiments are performed with cell cultures at 30 passages or lower.

Gene expression profiling: primary tumor versus dissociated culture

Microarray gene expression profiling and the PAM50 plus the claudin-low predictor (CLP) analysis [42, 44] were performed on all (six) DT cultures and available paired

Table 1 Classification of primary breast tumors at time of diagnosis

Sample	Receptors	Type of carcinoma
T13	ER−/PR−/H_2N+	Invasive ductal carcinoma
T19	ER−/PR−/H_2N+	Invasive ductal carcinoma
T21	ER−/PR−/H_2N+	Invasive ductal carcinoma
T22	ER−/PR−/H_2N−	Invasive ductal carcinoma with metaplastic features
T23	ER−/PR−/H_2N−	Invasive ductal carcinoma
T28	ER−/PR−/H_2N−	Invasive ductal carcinoma

primary tumors (5 of 6). The available triple-negative (TN) tumor samples, T22 was classified as basal/claudin-low, T23 as basal; T13 and T21 as Her2-enriched, and T19 as luminal A (Fig. 1b).

Interestingly, using this classification on the DT *cultures* shows that three different breast cancer subtypes are represented in the ER-negative DT cultures; DT13 is a Her2-enriched, DT22 to the basal/claudin-low, and DT28 to the basal subtype (Fig. 1b). Additionally, hierarchical cell line clustering analysis showed DT22 grouping with claudin-low cell lines such as MDA-MB-231; DT13 with Her2-enriched as SkBr3 and BT474, and DT28 with basal-epithelial cell lines such as the MDA-MB-468 [12]. On the other hand, DT19, DT21, and DT23 clustered together with reduction mammoplasty fibroblasts (RMFs) and MSCs rather than to their tumor of origin or with breast cancers or breast cancer cell lines (data not shown).

Paired gene expression scatter plots of all genes from the DT cells and their matching primary tumor shows a strong Pearson's correlation value between the basal/claudin-low DT22 ($r = 0.6864$) and the Her2+ DT13 ($r = 0.4566$) cultures and their corresponding primary tumors, indicating that these dissociated cultures retain a significant number of gene expression features found in the primary tumor. Cultures dissociated from tumors T19, T21, and T23 show very low correlation to the primary tumor of origin (Fig. 1c), which together with their similarity at the gene expression level with MSCs and CAFs led to different analysis than the other three cultures (DT13, DT22, and DT28) that clustered with breast cancer tumors and cell lines.

Morphology of breast cancer DT cultures in vitro

Cells within DT cultures exhibit unique morphologies varying in size, shape, and attachment to plastic. DT13 culture exhibited a high proportion of cells in suspension growing both as single round cell suspension as well as clusters that varied in size. On the other hand, DT22 cells grow as a mixture of mainly attached cells presenting a round cell body with long and thin spindles or a stellate-shape, with a low proportion of single cells growing in suspension. DT28 cells are adherent and have an epithelial-like morphology (Fig. 2a).

Growth rate and cell cycle profile of breast cancer DT cultures in vitro

Because these are short-term cultures of primary breast tumors, we were interested in determining their growth rate and cell cycle profile in vitro. This was performed using trypan blue dye exclusion assays to track cell number and measure viability every 48 h for 6 days. Doubling times ranged from 37 h (DT22) to 48 h (DT13 and DT28). Flow cytometric analysis of the cell cycle profile showed a %G1 ranging from 70 % (DT13) to 57 % (DT22 and DT28). The percent of S-phase ranged from 9 % (DT13) to 20 % (DT28) (Fig. 2b).

Expression of surface markers CD44 and CD24, mammosphere formation, and anchorage-independent growth by breast cancer DT cells

Since our cultures were isolated from primary breast tumors of different subtypes, we next explored the presence of cells with the $CD44^{+}/CD24^{-/lo}$ phenotype as they have been shown to have tumor-initiating properties [1] and to be enriched in tumors of the basal subtype [23]. In the breast cancer DT cultures, positive expression of CD44 was found in all DT cultures (Fig. 2c) while a strong expression of CD24 was only detected in DT28, thus displaying a $CD44^{+}/CD24^{+}$ phenotype. The CD44/CD24 expression phenotype for each DT was stable when examined over several passages. In addition, we performed mammosphere formation assays. When grown under low-attachment, serum-free, and low cellular density conditions, these DT cultures formed mammospheres with an efficiency ranging from 5 to 11 spheres per 10^4 cells (Fig. 2d).

Expression of ER, Her2, and EGFR in vitro

Expression of epithelial and mesenchymal markers, Her2, and EGFR was analyzed in lysates of asynchronously growing DT cells. As shown in Fig. 2e, levels of these proteins varied among DT cultures. Notably, DT28 exhibited the highest level of EGFR protein. Expression of vimentin was detected in DT22 and low to absent in DT13 and DT28. α-SMA was expressed in DT22 cells. Expression of cytokeratin 19 was found in DT13 and DT28 and absent in DT22. Her2 protein was only detected in DT13 cells (Fig. 2e).

Cloning of breast cancer DT cultures in soft agar

To determine whether DT cells have the ability to grow in an anchorage-independent manner, colony formation in

a

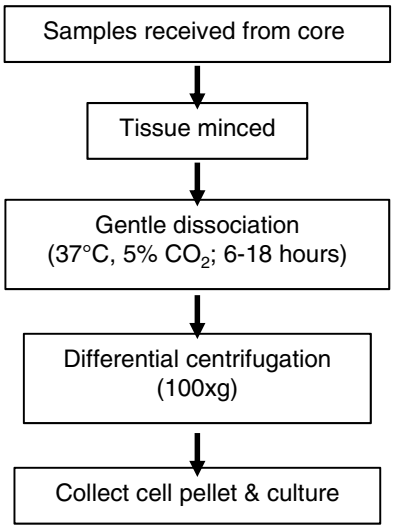

b

Primary Tumor		Dissociated Culture	
Sample	PAM50 + CLP Subtype	Sample	PAM50 + CLP Subtype
T13	Her2	DT13	Her2
T19	LumA	DT19	Basal/Claudin
T21	Her2	DT21	Basal/Claudin
T22	Basal/Claudin	DT22	Basal/Claudin
T23	Basal	DT23	Basal/Claudin
T28	NA	DT28	Basal

c

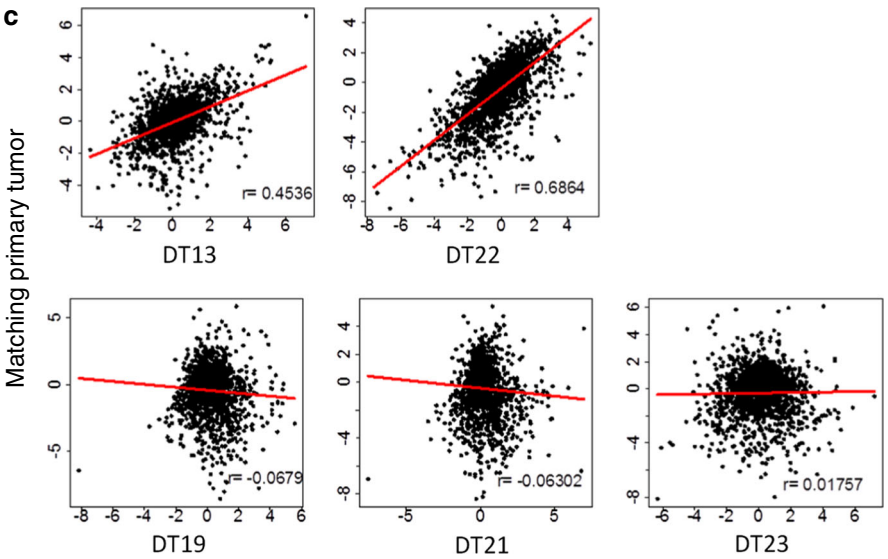

Fig. 1 Generation of dissociated tumor cell cultures (DTs) and their gene expression profiling. **a** Schematic representation of gentle dissociation protocol for generation of dissociated tumor cells. **b** Table summarizing PAM50 + CLP results for primary tumor and matching dissociated culture. **c** Pairwise gene expression scatter plots of dissociated cultures and available matching primary tumors

soft agar was determined for up to 8 weeks. As shown in Fig. 2f, by 8 weeks, colonies were detected in DT13, DT22, and DT28 with the largest colonies formed by DT22, followed by DT28 and DT13.

Tumor formation by DT cells in NOD/SCID mice

Having determined that our breast cancer DT cultures had the ability to clone in soft agar, we next determined their tumorigenic potential by injecting cells into the mammary fat pad of 6- to 8-week-old female NOD/SCID mice. Consistent with the soft agar colony formation assay results, all three DT cultures were tumorigenic in NOD/SCID mice. The resulting tumor growth curves are shown in Fig. 3a. Tumor latency periods (i.e., palpable tumors detected) ranged from 2 to 10 days post-inoculation. The average tumor weights ranged from 0.06 to 2.2 g (Fig. 3b), with the smallest tumors generated by DT13 and the largest generated by DT22. For the former, tumors reached a growth plateau around week 4 when the estimated volume was about 50–60 mm^3. While no further increase was detected thereafter, tumors did not regress and remained stable for up to at least 16 weeks after injection when the experiment was terminated. The gross pathology of the tumors generated by DT28 (basal) had

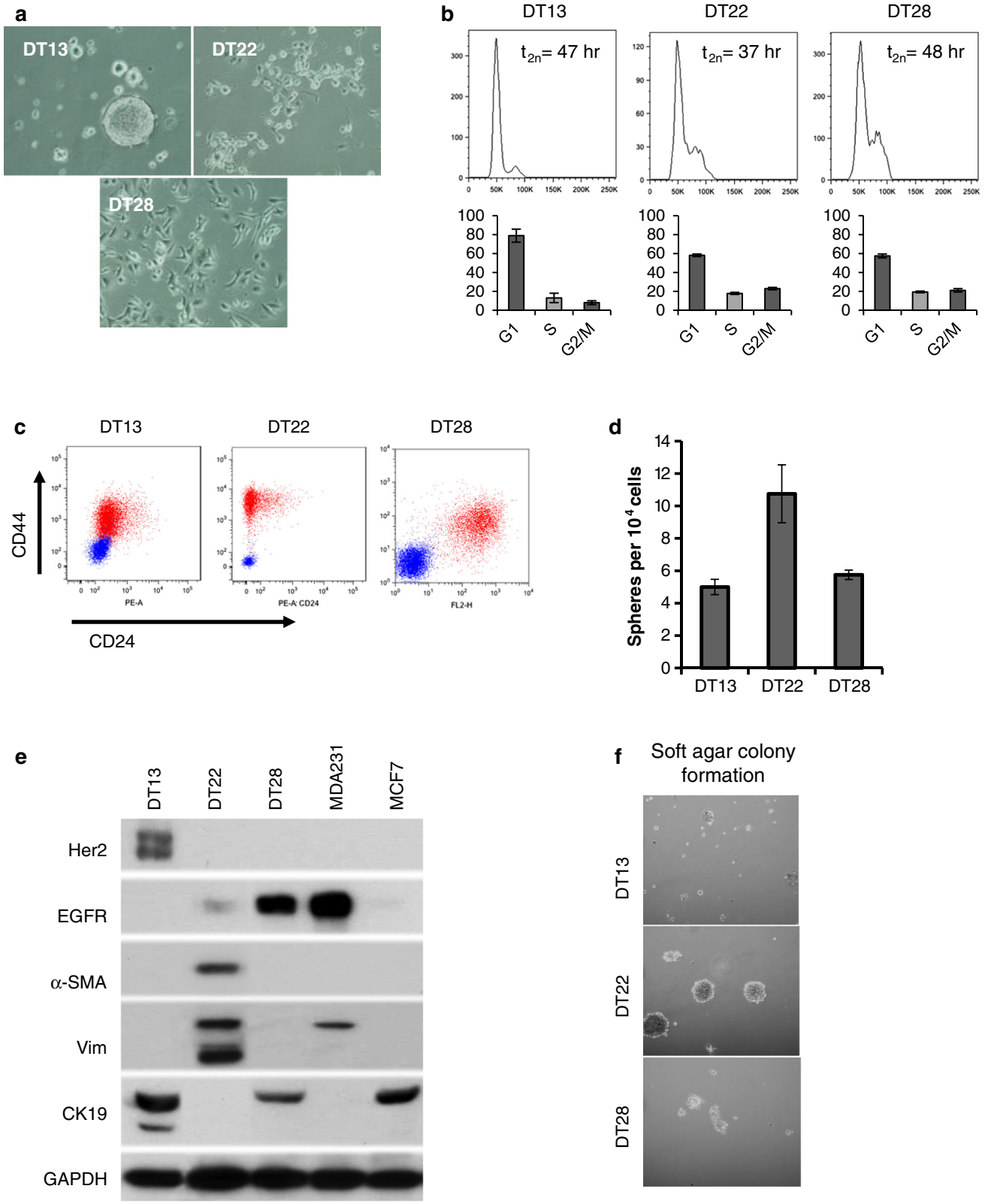

Fig. 2 In vitro features of DT cultures. **a** Morphology of DT cells in 2D culture. **b** Doubling time and cell cycle distribution. **c** CD44/CD24 expression (isotype control: *blue dots*; labeled cells: *red dots*). **d** Representative images of colony formation in soft agar (4 weeks). **e** Lysates of asynchronous DT cultures were analyzed by western blot for expression of the indicated proteins

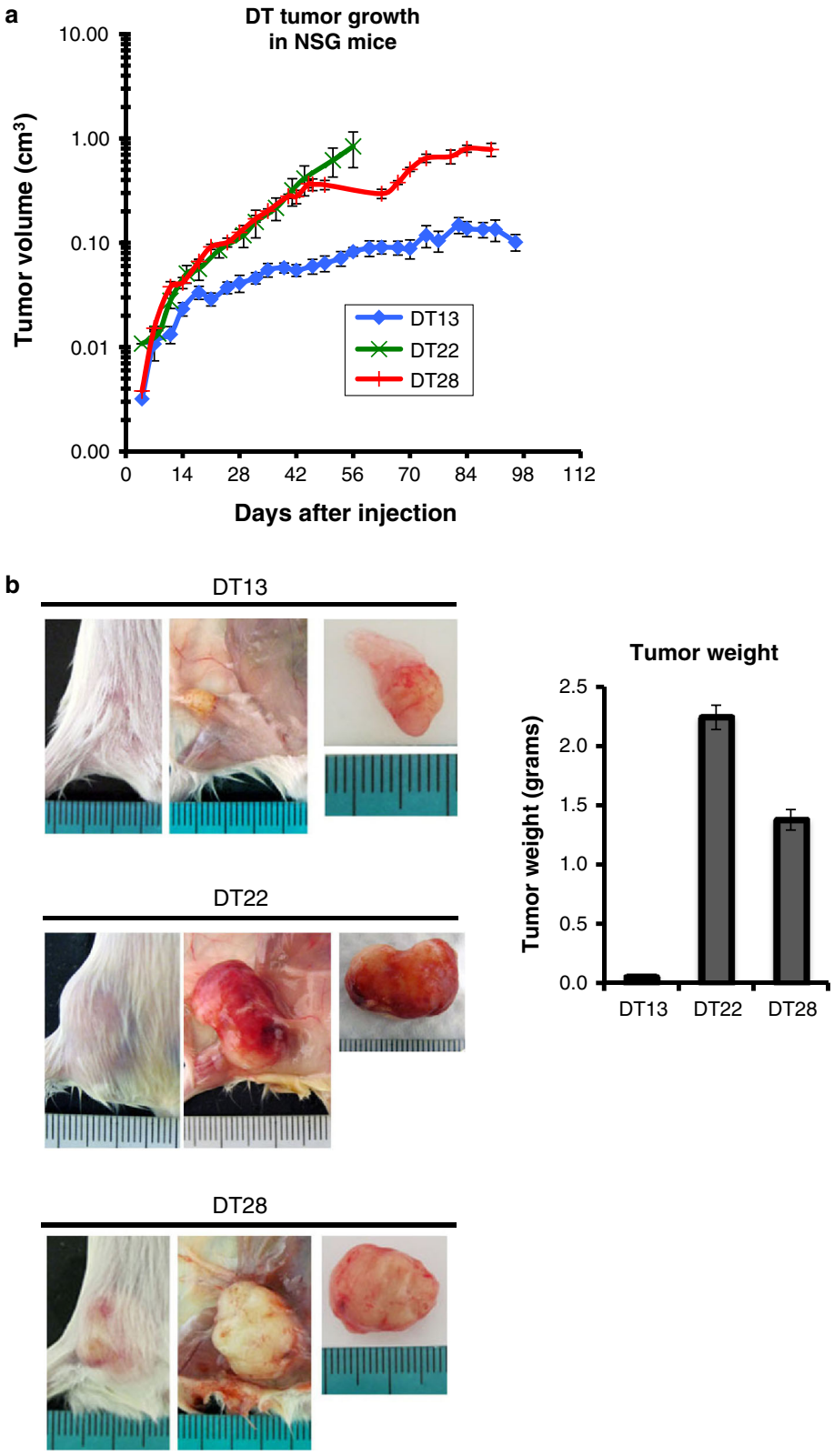

Fig. 3 Tumorigenic ability of DT cells in NOD/SCID mice. **a** Tumor growth curves of 1×10^6 DT cells injected into the mammary fat pad of NOD/SCID mice (*left panel*) and average endpoint tumor weight (*right panel*). **b** Representative images of gross observation of primary tumors in situ and excised

geographic or irregular necrosis, and a pushing edge locally invading into the skeletal muscle. In addition, these tumors attached to and caused necrosis to the skin. The large tumors generated by DT22 cells did not cause a necrotic process on the surface of the skin and tumors displayed a smooth, well-circumscribed border (Fig. 3b).

Immunohistochemical analysis of xenografted DT tumors

Sections from xenografted DT primary tumors were stained with antibodies against human Ki67, EGFR, Her2, CK5, CK14, and CK18. The luminal keratin CK18 and basal keratins CK5 and CK14 were detected in DT13 and DT28 tumors, but not in DT22 (Fig. 4a). IHC analysis of Ki67 showed positive cells in all tumors, and consistent with each tumor's architecture, those with geographic necrosis—DT28—showed Ki67+ cells in the pushing edge, as well as throughout the non-necrotic DT22 tumors. The expression of EGFR was highest in DT28 and DT13 tumors, and the remaining tumor exhibited only a few—to none—cells expressing EGFR. Consistent with the in vitro expression of Her2 in DT13 cells, a strong expression of Her2 was also detected in DT13 tumors (Fig. 4b).

Spontaneous metastasis of DT28 cells in NOD/SCID and NSG mice

When injected into the mammary fat pad of NOD/SCID mice, DT28 (basal) cells formed spontaneous metastasis from the orthotopic site to lymph nodes and lung. This was achieved without primary tumor excision or direct inoculation into the host circulation. DT 28 cells metastasized to lungs and axillary lymph nodes of 64 % of the animals (Fig. 5a). In addition to the H&E staining of the metastatic lesions, IHC of CK18 confirms the presence of the DT28 cells (Fig. 5b).

We have recently shown that NOD SCID gamma null (NSG) mice exhibit a high frequency of metastasis when breast cancer cells are injected orthotopically into the mammary fat pad [26]. This was also observed with DT cultures when compared to their metastatic ability in NOD/SCID mice. Tumorigenic DT cultures formed tumors in NSG mice (Fig. 6a), and the one that had previously metastasized in NOD/SCID also did so in NSG mice; however, the metastatic frequency was increased to 100 %. Importantly, the organ tropism of the DT culture for the establishment of metastatic lesions was the same in NOD/SCID and NSG mice even though the frequency was significantly increased (Fig. 6b). As observed in NOD/SCID mice, no metastatic lesions from DT13 or DT22 tumors could be detected in NSG mice while DT28 metastasized to lymph nodes and lung (Fig. 6c).

DT19, DT21, and DT23 are cellular models of CAFs

As mentioned above, the gene expression analysis of DT19, DT21, and DT23 showed that these three DT cultures did not cluster with their paired primary tumor nor breast cancer cell lines, and rather clustered with RMFs and MSCs. This prompted the further characterization of these cultures to determine whether they are CAFs. They have fibroblast-like morphology displaying branched cytoplasm (Fig. 7a). A strong correlation was seen in paired gene expression scatter plots of DT19, DT21, and DT23 compared to RMFs and MSCs (Fig. 7b). Using MCF-7 cells as a control for epithelial markers, and HMFs as a normal fibroblast control, we found this group of DTs to show positive expression of FAP, alpha smooth muscle actin (α-SMA), and vimentin, while lacking epithelial markers such as cytokeratins. FAP, a marker of CAFs, was found only in the DT19, DT21, and DT23 cells and not in HMFs. These results were confirmed using both immunofluorescence staining and western blot analyses (Fig. 7c). The three DT cultures exhibit expression of the stromal marker CD44 and lack of expression of epithelial surface antigen (ESA) by flow cytometry (Fig. 7d). While these DTs have sphere-forming ability in mammosphere formation assays (Fig. 7e), they do not form colonies in soft agar nor tumors in NOD/SCID mice (Fig. 7f). However, they do have the ability to enhance the formation of colonies in soft agar of the tumorigenic DT cells where these CAF-like DT cultures were co-cultured with DT12, DT22, and DT28 cells and colony formation assessed at 2 weeks, a time prior to significant colony formation by cancer cells alone (Fig. 7g). Collectively, these data indicate that DT19, DT21, and DT23 are cultures of CAFs isolated from three different subtypes of breast primary tumors: a luminal A, an ER−/PR−/H_2N+, and TN, respectively.

Discussion

Here, we describe the characterization of cell cultures generated by dissociation of eight different primary breast tumors by means of a gentle enzymatic dissociation and differential centrifugation protocol. From the DTs, we obtained "dissociated tumor (DT) cell cultures" of growing, propagating cultures with 100 % rate of success.

Over the past decade, great efforts have been made by several groups to further dissect the classification of breast cancer with the aid of genomic-based bioinformatic analysis. Knowledge of breast cancer subtypes, correlation with clinico-pathological features and response to current treatments by means of genomic studies and profiling has been significantly increased and has allowed a better understanding of the heterogeneity of this disease [43, 44, 52]. In this study, available samples of the original tumors and the resulting DT culture grown in vitro were classified by the PAM50 plus the claudin-low predictor (CLP) analysis [42, 44]. This confirmed both ER−/PR−/Her2+ tumors as such. With regards to the cultures originated from TNBC, the PAM50 classification was consistent with the initial clinical diagnosis and were all classified as basal.

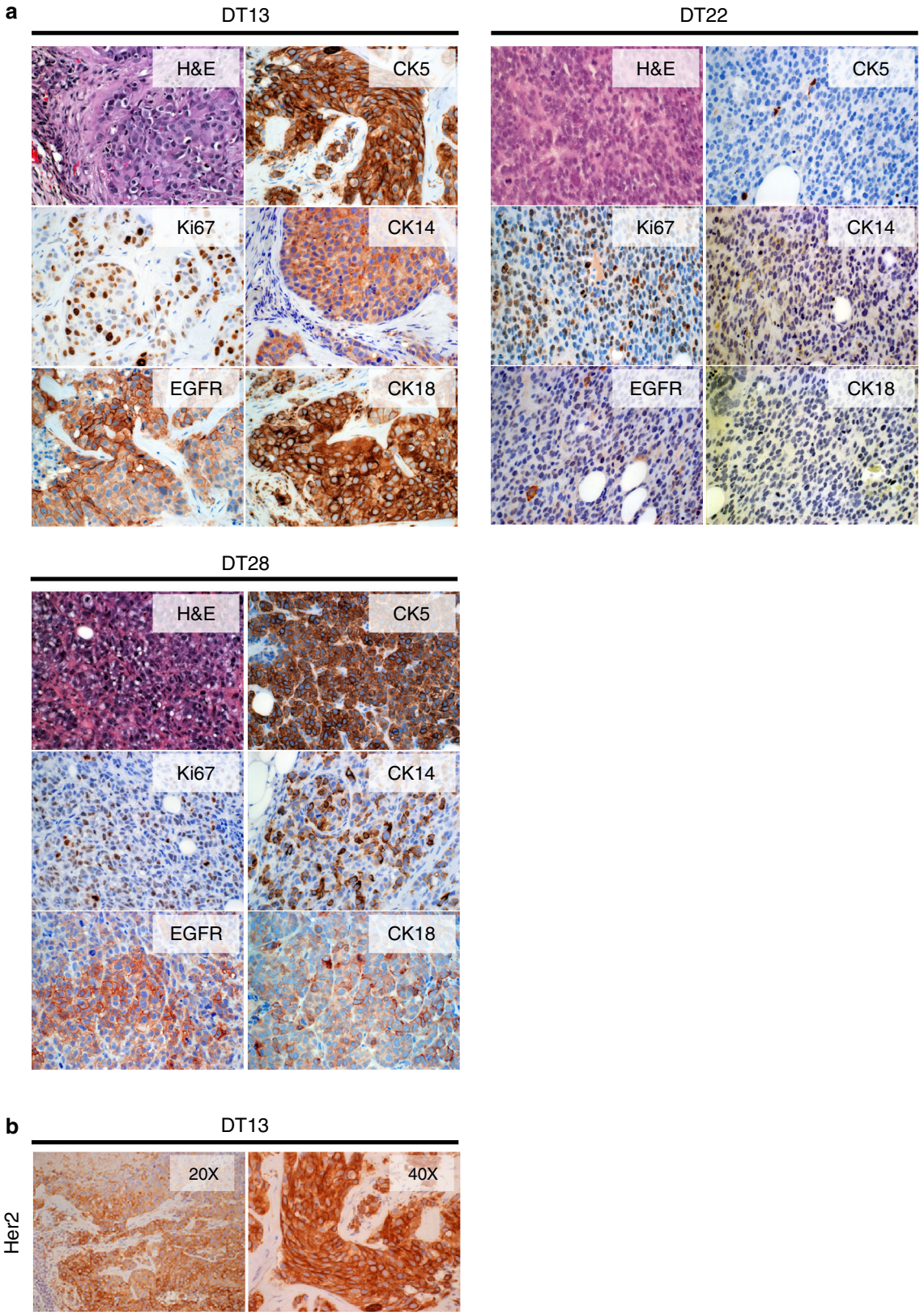

Fig. 4 Histopathological analysis of xenografted DT primary tumors. **a** Representative images of DT mammary tumors characterized by histopathologic and immunohistochemical stainings including H&E, the proliferation marker Ki67, epidermal growth factor receptor (EGFR), cytokeratin 5 (CK5), cytokeratin 14 (CK14), and cytokeratin 18 (CK18); and **b** human epidermal growth factor receptor 2 (Her2) was confirmed for DT13

a DT28 (NOD scid)

Metastatic site	Frequency
Lung	64% (7/11)
Lymph nodes	27% (3/11)
Total mice with metastatic disease	64% (7/11)

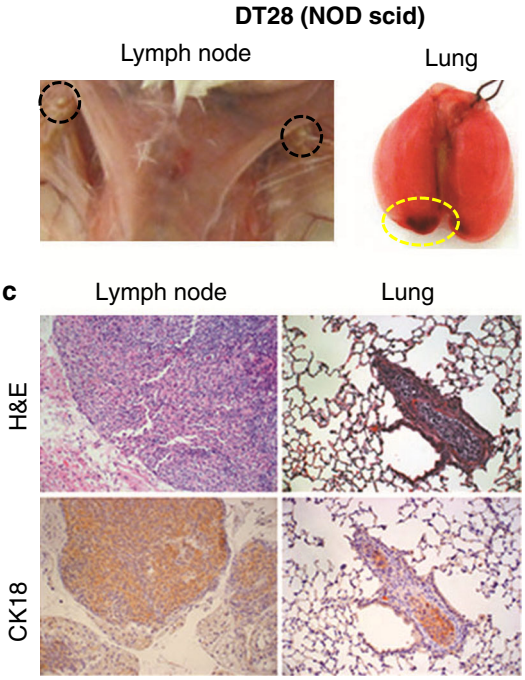

Fig. 5 DT28 cells are metastatic in NOD/SCID. **a** Metastatic sites and frequency of D28 cells in NOD/SCID mice; **b** images of gross observation of lung and lymph node metastases, **c** H&E and immunohistochemical staining (EGFR and CK5) confirming the presence of DT28 cells in secondary sites. Metastatic lesions are indicated by *yellow-dashed circle*

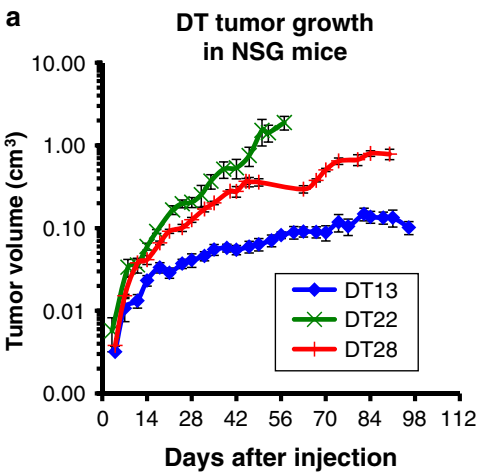

b

DT culture	Metastatic site	Frequency
DT13	Not detected	N/A
DT22	Not detected	N/A
DT28	Lung	100%
	Lymph nodes	100%

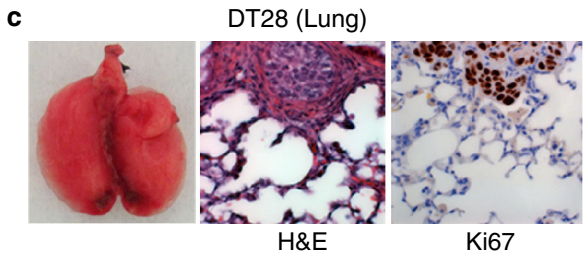

Fig. 6 Metastatic frequency of DT cells is increased in NSG mice. **a** Tumor growth curves of DT cells injected into the mammary fat pad of NSG mice. **b** Metastatic sites and frequency of DT28 cells in NSG mice. **c** Representative images of gross observation of tumors and metastatic lesions in situ and excised

A variety of morphological features were observed in the tumorigenic DT cultures, ranging from spindled cells to mixed cultures of both attached and floating cells to other cells growing exclusively as suspensions. In vitro, expression of luminal cytokeratins was detected in DT13 and DT28 (CK19 and CK18 positive). In the remaining DT culture, DT22, expression of these cytokeratins was not detected by western blot. Loss of cytokeratins in those

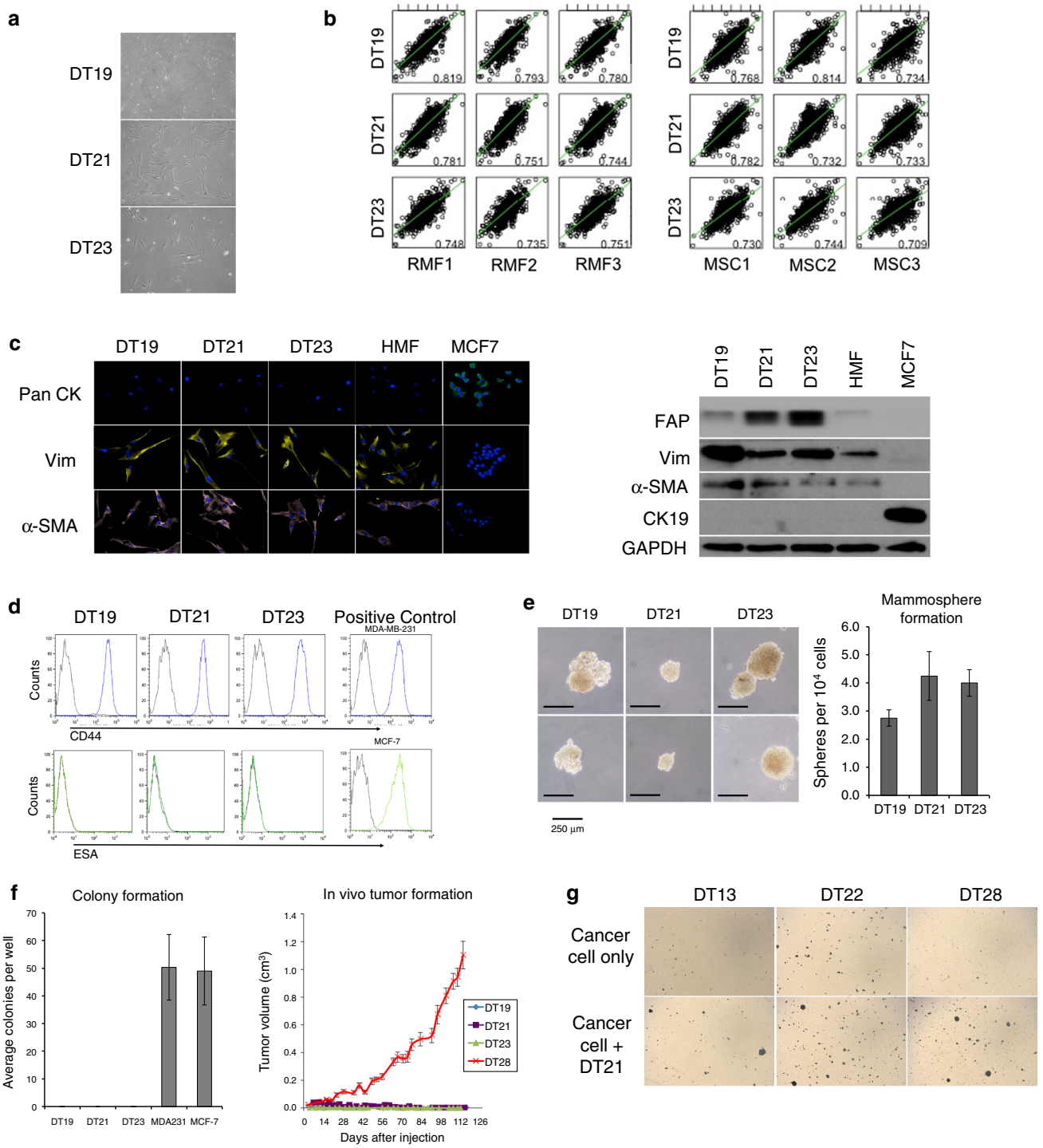

Fig. 7 Stromal cell cultures DT19, DT21, and DT23. **a** Fibroblast-like morphology of DT19, DT21, and DT23. **b** Pairwise gene expression of DT19, DT21, and DT23 to RMFs and MSCs from the UNC dataset. **c** Expression of cytokeratins, vimentin, and α-SMA as detected by immunofluorescence (*upper panel*) and CK19, vimentin (vim), FAP, and α-SMA by western blot (*lower panel*). **d** Expression of CD44 and ESA was detected by flow cytometry. **e** Representative pictures of mammospheres and average count per 10^4 cells (*bars* are average of three independent experiments ±SEM). **f** Colony formation ability of DT19, DT21, and DT23 was compared to that of MDA-MB231 and MCF7 cells; 1×10^6 cells were injected into the mammary fat pads of NOD/SCID mice and tumor formation monitored for the indicated time and DT28 tumor growth is used as a positive control. **g** Cloning ability of DT13, DT22, and DT28 was enhanced when co-cultured with DT21 (1:3 ratio)

cultures is not entirely surprising since reduction of epithelial markers can be a common feature of basal-like and claudin-low breast cancers [44], and as part of an ongoing EMT process [32, 58]. Consistent with this, expression of the mesenchymal marker vimentin was detected in the DT22 culture, which lacks cytokeratins. Interestingly, this marker was highest in the DT defined by PAM50 as basal and clustering to claudin-low cell lines (DT22), in agreement with what has been previously described for claudin-low tumors [21, 44]. Increased expression of mesenchymal markers including α-SMA has also been associated with basal breast cancer [27, 49]. Among our TN cultures, α-SMA was absent in those cultures growing in suspension or with an epithelial morphology while being expressed by DT22 (claudin-low), which is the culture with the highest proportion spindled, stellate-shape cells and was dissociated from a primary tumor exhibiting metaplastic features.

All three DT cultures described by gene expression analysis as breast cancer cells formed tumors when orthotopically injected into the mammary fat pad of NOD/SCID and NSG mice. Growth rate, metastatic ability, gross pathology, and immunohistochemical features varied among DTs. Individual features of these cultures include the strong expression of Her2 by DT13, and of EGFR in DT28 cells in vitro as well as in an in vivo setting. Importantly, 1 of 3 DT cultures developed spontaneous metastasis from orthotopically implanted tumors in NOD/SCID mice with a metastatic frequency ranging around 64 %. Lesions were found in lymph nodes and lungs, which are common sites of metastasis observed in breast cancer patients [59].

Our group has recently reported that NSG mice consistently develop macrometastasis when established breast cancer cell lines were injected in the orthotopic site [26]. This was also observed when the DT cultures were injected into the mammary fat pads of NSG mice. Compared to NOD/SCID mice, NSG mice showed a higher frequency of metastasis and, importantly, the organ tropism previously observed in the NOD/SCID mice was maintained in the NSG model. On the one hand, these results suggest that breast cancer cells may have an innate ability or tropism to metastasize to a given tissue, which is in agreement with previous studies reporting organ-specific gene signatures within primary breast tumors to metastasize to brain [10], bone [35], and lung [36]. Previous reports in the literature, where similar experiments of orthotopic injections of MDA-MB-231 cells into the mammary fat pads of Nude mice showed that macroscopic lung metastases formed in only 1 of 7 mice 20 weeks post-injection [45]. Therefore, numerous studies have relied on putting these cells in circulation to study the metastatic process, rather than allowing the metastases to form from an orthotopically implanted tumor [34, 36]. We do not rule out the possibility that DT cells could also metastasize to other organs commonly invaded by breast cancer cells such as the bone and brain in the mouse models described herein or others such as the Rag2−/− IL2g−/− mouse model, which has recently been reported to exhibit multi-organ metastatic spread from orthotopically injected Her2+ breast cancer cells [38].

Interactions between stromal and epithelial cells have been shown to play pivotal roles in tumor progression and metastatsis [19, 31]. In this study, we have also generated a group of primary breast tumor-derived CAFs isolated from three different tumor subtypes; a luminal A, an ER−/PR/Her2+, and a TN breast tumor. In addition to expressing markers such as α-SMA and CD44 and lacking epithelial markers (cytokeratins and ESA), these three DTs express FAP, a marker of activated fibroblasts [18]. Mammosphere and tumor formation assays as well as microarray studies indicate that while DT19, DT21, and DT23 can form robust mammospheres, they are not able to form colonies in soft agar nor tumors in mice, and that they share significant gene expression similarities to MSCs and RMFs rather than to the breast tumor of origin or to other breast cancers or breast cancer cell lines. CAFs are a heterogeneous population of cells, and have been reported to arise from both MSCs and activation of normal fibroblasts [5, 46]. Based on expression of α-SMA, chondroitin sulfate neural glial proteoglycan (NG2), FAP and FSP two subpopulations of CAFs have been recently described: activated myofibroblasts (α-SMA+, NG2+) and activated fibroblasts (FAP+ and FSP+) [54]. Since the DT CAF cultures share gene expression and protein expression of both MSCs and RMFs they may possibly be comprised of both of these populations. Further studies into the generation of these CAFs, in particular, cell of origin, and role of these in breast cancer biology are ongoing. For this purpose, DT19, DT21, and DT23 will be here onto referred as to CAF19-LA, CAF21-Her2, and CAF23-TN, respectively.

Table 2 Summary of DT cellular models: tumorigenic and CAF cell cultures

Tumorigenic DT cultures			CAF DT cultures		
DT culture	PAM50 subtype	Metastasis	DT culture	Tumor of origin	Proposed name
DT13	Her2-enriched (ER−)	NO	DT19	Luminal A	CAF19-LA
DT22	Basal (claudin-low)	NO	DT21	Her2-enriched	CAF21-H_2N
DT28	Basal (basal-epithelial)	Lung Lymph node	DT23	Basal	CAF23-TN

In summary, our panel of DT cultures consists of two groups of cellular models; one comprising tumorigenic and metastatic breast cancer cells and another group formed by CAFs, shown in Table 2. CAFs are a pivotal component of the TME, and thus cellular models such as those herein described are crucial for the better understanding of interactions within primary breast tumors. The tumorigenic DTs retain important markers in breast cancer biology—such as EGFR and Her2—in both the in vitro and in vivo settings, and exhibit significant gene expression similarities to their paired primary tumor. Our DT cultures are of varying molecular subtypes, and thus, use of these tumorigenic and CAF cultures (individually or in combination) provides valuable models for the study of breast cancer pathogenesis including metastatic spread, in vivo assessment of drug sensitivities, and discovery of novel therapeutics.

Acknowledgments This project was supported by the NIH Grant 1R01 CA113674 and The Bankhead Coley Cancer Research Program Pre SPORE Grant 09BW-04 to DEA. Award Number T32CA119929 from the National Cancer Institute supported KDE. The content is solely the responsibility of the authors and does not necessarily represent the official views of the National Cancer Institute or the National Institute of Health. This project was also supported by the BCRF funds to MEL. The authors would like to thank Ms. Sonja Dean and Dr. Ayse Burcu Ergonul (University of Miami) and Dr. James Rae (University of Michigan) for valuable discussions.

References

1. Al-Hajj M, Wicha MS, Benito-Hernandez A, Morrison SJ, Clarke MF (2003) Prospective identification of tumorigenic breast cancer cells. Proc Natl Acad Sci USA 100:3983–3988
2. Amano H, Hayashi I, Endo H, Kitasato H, Yamashina S, Maruyama T et al (2003) Host prostaglandin E(2)-EP3 signaling regulates tumor-associated angiogenesis and tumor growth. J Exp Med 197:221–232
3. Augsten M, Hagglof C, Olsson E, Stolz C, Tsagozis P, Levchenko T et al (2009) CXCL14 is an autocrine growth factor for fibroblasts and acts as a multi-modal stimulator of prostate tumor growth. Proc Natl Acad Sci USA 106:3414–3419
4. Bastien RR, Rodriguez-Lescure A, Ebbert MT, Prat A, Munarriz B, Rowe L et al (2012) PAM50 breast cancer subtyping by RT-qPCR and concordance with standard clinical molecular markers. BMC Med Genomics 5:44
5. Battula VL, Evans KW, Hollier BG, Shi Y, Marini FC, Ayyanan A et al (2010) Epithelial–mesenchymal transition-derived cells exhibit multilineage differentiation potential similar to mesenchymal stem cells. Stem Cells 28:1435–1445
6. Bayliss J, Hilger A, Vishnu P, Diehl K, El-Ashry D (2007) Reversal of the estrogen receptor negative phenotype in breast cancer and restoration of antiestrogen response. Clin Cancer Res 13:7029–7036
7. Bayraktar UD, Kim TK, Drews-Elger K, Benjamin C, El-Ashry D, Wieder E et al (2011) Simultaneous measurement of ERalpha, HER2, and phosphoERK1/2 in breast cancer cell lines by flow cytometry. Breast Cancer Res Treat 129:623–628
8. Bhowmick NA, Neilson EG, Moses HL (2004) Stromal fibroblasts in cancer initiation and progression. Nature 432:332–337
9. Boire A, Covic L, Agarwal A, Jacques S, Sherifi S, Kuliopulos A (2005) PAR1 is a matrix metalloprotease-1 receptor that promotes invasion and tumorigenesis of breast cancer cells. Cell 120:303–313
10. Bos PD, Zhang XH, Nadal C, Shu W, Gomis RR, Nguyen DX et al (2009) Genes that mediate breast cancer metastasis to the brain. Nature 459:1005–1009
11. Burdall SE, Hanby AM, Lansdown MR, Speirs V (2003) Breast cancer cell lines: friend or foe? Breast Cancer Res 5:89–95
12. Cailleau R, Young R, Olive M, Reeves WJ Jr (1974) Breast tumor cell lines from pleural effusions. J Natl Cancer Inst 53:661–674
13. Carey LA, Dees EC, Sawyer L, Gatti L, Moore DT, Collichio F et al (2007) The triple negative paradox: primary tumor chemosensitivity of breast cancer subtypes. Clin Cancer Res 13:2329–2334
14. Cheang MC, Voduc KD, Tu D, Jiang S, Leung S, Chia SK et al (2012) Responsiveness of intrinsic subtypes to adjuvant anthracycline substitution in the NCIC.CTG MA.5 randomized trial. Clin Cancer Res 18:2402–2412
15. Fan C, Oh DS, Wessels L, Weigelt B, Nuyten DS, Nobel AB et al (2006) Concordance among gene-expression-based predictors for breast cancer. N Engl J Med 355:560–569
16. Fantozzi A, Christofori G (2006) Mouse models of breast cancer metastasis. Breast Cancer Res 8:212
17. Francia G, Cruz-Munoz W, Man S, Xu P, Kerbel RS (2011) Mouse models of advanced spontaneous metastasis for experimental therapeutics. Nat Rev Cancer 11:135–141
18. Garin-Chesa P, Old LJ, Rettig WJ (1990) Cell surface glycoprotein of reactive stromal fibroblasts as a potential antibody target in human epithelial cancers. Proc Natl Acad Sci USA 87:7235–7239
19. Hanahan D, Coussens LM (2012) Accessories to the crime: functions of cells recruited to the tumor microenvironment. Cancer Cell 21:309–322
20. Hanahan D, Weinberg RA (2011) Hallmarks of cancer: the next generation. Cell 144:646–674
21. Herschkowitz JI, Simin K, Weigman VJ, Mikaelian I, Usary J, Hu Z et al (2007) Identification of conserved gene expression features between murine mammary carcinoma models and human breast tumors. Genome Biol 8:R76
22. Hess KR, Pusztai L, Buzdar AU, Hortobagyi GN (2003) Estrogen receptors and distinct patterns of breast cancer relapse. Breast Cancer Res Treat 78:105–118
23. Honeth G, Bendahl PO, Ringner M, Saal LH, Gruvberger-Saal SK, Lovgren K et al (2008) The $CD44^{+}/CD24^{-}$ phenotype is enriched in basal-like breast tumors. Breast Cancer Res 10:R53
24. Hu Z, Fan C, Oh DS, Marron JS, He X, Qaqish BF et al (2006) The molecular portraits of breast tumors are conserved across microarray platforms. BMC Genom 7:96
25. Ikeda Y, Hayashi I, Kamoshita E, Yamazaki A, Endo H, Ishihara K et al (2004) Host stromal bradykinin B2 receptor signaling facilitates tumor-associated angiogenesis and tumor growth. Cancer Res 64:5178–5185
26. Iorns E, Drews-Elger K, Ward TM, Dean S, Clarke J, Berry D et al (2012) A new mouse model for the study of human breast cancer metastasis. PLoS ONE 7:e47995
27. Jeong H, Ryu YJ, An J, Lee Y, Kim A (2012) Epithelial–mesenchymal transition in breast cancer correlates with high histological grade and triple-negative phenotype. Histopathology 60:E87–E95
28. Jessani N, Humphrey M, McDonald WH, Niessen S, Masuda K, Gangadharan B et al (2004) Carcinoma and stromal enzyme activity profiles associated with breast tumor growth in vivo. Proc Natl Acad Sci USA 101:13756–13761

29. Kalluri R, Zeisberg M (2006) Fibroblasts in cancer. Nat Rev Cancer 6:392–401
30. Kao J, Salari K, Bocanegra M, Choi YL, Girard L, Gandhi J et al (2009) Molecular profiling of breast cancer cell lines defines relevant tumor models and provides a resource for cancer gene discovery. PLoS ONE 4:e6146
31. Karnoub AE, Dash AB, Vo AP, Sullivan A, Brooks MW, Bell GW et al (2007) Mesenchymal stem cells within tumour stroma promote breast cancer metastasis. Nature 449:557–563
32. Kokkinos MI, Wafai R, Wong MK, Newgreen DF, Thompson EW, Waltham M (2007) Vimentin and epithelial–mesenchymal transition in human breast cancer—observations in vitro and in vivo. Cells Tissues Organs 185:191–203
33. Kuperwasser C, Chavarria T, Wu M, Magrane G, Gray JW, Carey L et al (2004) Reconstruction of functionally normal and malignant human breast tissues in mice. Proc Natl Acad Sci USA 101:4966–4971
34. Minn AJ, Gupta GP, Siegel PM, Bos PD, Shu W, Giri DD et al (2005) Genes that mediate breast cancer metastasis to lung. Nature 436:518–524
35. Minn AJ, Kang Y, Serganova I, Gupta GP, Giri DD, Doubrovin M et al (2005) Distinct organ-specific metastatic potential of individual breast cancer cells and primary tumors. J Clin Invest 115:44–55
36. Minn AJ, Gupta GP, Padua D, Bos P, Nguyen DX, Nuyten D et al (2007) Lung metastasis genes couple breast tumor size and metastatic spread. Proc Natl Acad Sci USA 104:6740–6745
37. Mueller MM, Fusenig NE (2004) Friends or foes—bipolar effects of the tumour stroma in cancer. Nat Rev Cancer 4:839–849
38. Nanni P, Nicoletti G, Palladini A, Croci S, Murgo A, Ianzano ML et al (2012) Multiorgan metastasis of human HER-2+ breast cancer in Rag2−/−; Il2rg−/− mice and treatment with PI3K inhibitor. PLoS ONE 7:e39626
39. Orimo A, Weinberg RA (2006) Stromal fibroblasts in cancer: a novel tumor-promoting cell type. Cell Cycle 5:1597–1601
40. Orimo A, Gupta PB, Sgroi DC, Arenzana-Seisdedos F, Delaunay T, Naeem R et al (2005) Stromal fibroblasts present in invasive human breast carcinomas promote tumor growth and angiogenesis through elevated SDF-1/CXCL12 secretion. Cell 121:335–348
41. O'Toole SA, Beith JM, Millar EK, West R, McLean A, Cazet A et al (2013) Therapeutic targets in triple negative breast cancer. J Clin Pathol 66:530–542
42. Parker JS, Mullins M, Cheang MC, Leung S, Voduc D, Vickery T et al (2009) Supervised risk predictor of breast cancer based on intrinsic subtypes. J Clin Oncol 27:1160–1167
43. Perou CM, Sorlie T, Eisen MB, van de Rijn M, Jeffrey SS, Rees CA et al (2000) Molecular portraits of human breast tumours. Nature 406:747–752
44. Prat A, Parker JS, Karginova O, Fan C, Livasy C, Herschkowitz JI et al (2010) Phenotypic and molecular characterization of the claudin-low intrinsic subtype of breast cancer. Breast Cancer Res 12:R68
45. Price JE, Polyzos A, Zhang RD, Daniels LM (1990) Tumorigenicity and metastasis of human breast carcinoma cell lines in nude mice. Cancer Res 50:717–721
46. Radisky DC, Kenny PA, Bissell MJ (2007) Fibrosis and cancer: do myofibroblasts come also from epithelial cells via EMT? J Cell Biochem 101:830–839
47. R-Core-Team (2013) R: a language and environment for statistical computing. R Foundation for Statistical Computing, Vienna
48. Rouzier R, Perou CM, Symmans WF, Ibrahim N, Cristofanilli M, Anderson K et al (2005) Breast cancer molecular subtypes respond differently to preoperative chemotherapy. Clin Cancer Res 11:5678–5685
49. Sarrio D, Rodriguez-Pinilla SM, Hardisson D, Cano A, Moreno-Bueno G, Palacios J (2008) Epithelial–mesenchymal transition in breast cancer relates to the basal-like phenotype. Cancer Res 68:989–997
50. Shekhar MP, Santner S, Carolin KA, Tait L (2007) Direct involvement of breast tumor fibroblasts in the modulation of tamoxifen sensitivity. Am J Pathol 170:1546–1560
51. Siegel R, Naishadham D, Jemal A (2012) Cancer statistics, 2012. CA Cancer J Clin 62:10–29
52. Sorlie T, Perou CM, Tibshirani R, Aas T, Geisler S, Johnsen H et al (2001) Gene expression patterns of breast carcinomas distinguish tumor subclasses with clinical implications. Proc Natl Acad Sci USA 98:10869–10874
53. Sorlie T, Tibshirani R, Parker J, Hastie T, Marron JS, Nobel A et al (2003) Repeated observation of breast tumor subtypes in independent gene expression data sets. Proc Natl Acad Sci USA 100:8418–8423
54. Spaeth EL, Labaff AM, Toole BP, Klopp A, Andreeff M, Marini FC (2013) Mesenchymal CD44 expression contributes to the acquisition of an activated fibroblast phenotype via TWIST activation in the tumor microenvironment. Cancer Res 73:5347–5359
55. Speirs V, Green AR, Walton DS, Kerin MJ, Fox JN, Carleton PJ et al (1998) Short-term primary culture of epithelial cells derived from human breast tumours. Br J Cancer 78:1421–1429
56. Sternlicht MD, Lochter A, Sympson CJ, Huey B, Rougier JP, Gray JW et al (1999) The stromal proteinase MMP3/stromelysin-1 promotes mammary carcinogenesis. Cell 98:137–146
57. Straussman R, Morikawa T, Shee K, Barzily-Rokni M, Qian ZR, Du J et al (2012) Tumour micro-environment elicits innate resistance to RAF inhibitors through HGF secretion. Nature 487:500–504
58. Tomaskovic-Crook E, Thompson EW, Thiery JP (2009) Epithelial to mesenchymal transition and breast cancer. Breast Cancer Res 11:213
59. Weigelt B, Peterse JL, van't Veer LJ (2005) Breast cancer metastasis: markers and models. Nat Rev Cancer 5:591–602
60. Williams CS, Tsujii M, Reese J, Dey SK, DuBois RN (2000) Host cyclooxygenase-2 modulates carcinoma growth. J Clin Invest 105:1589–1594